frontiers in Materials

ORIGINAL RESEARCH
published: 03 December 2019
doi: 10.3389/fmats.2019.00311

Removing Polymeric Coatings With Nanostructured Fluids: Influence of Substrate, Nature of the Film, and Application Methodology

Michele Baglioni, Margherita Alterini, David Chelazzi, Rodorico Giorgi and Piero Baglioni**

Department of Chemistry and CSGI, University of Florence, Sesto Fiorentino, Italy

OPEN ACCESS

Edited by:
Luca Tortora,
Roma Tre University, Italy

Reviewed by:
Claudia Mazzuca,
University of Rome Tor Vergata, Italy
Nunzio Tuccitto,
University of Catania, Italy

***Correspondence:**
Rodorico Giorgi
giorgi@csgi.unifi.it
Piero Baglioni
baglioni@csgi.unifi.it

Specialty section:
This article was submitted to Colloidal Materials and Interfaces, a section of the journal Frontiers in Materials

Received: *25 September 2019*
Accepted: *18 November 2019*
Published: *03 December 2019*

Citation:
Baglioni M, Alterini M, Chelazzi D, Giorgi R and Baglioni P (2019) Removing Polymeric Coatings With Nanostructured Fluids: Influence of Substrate, Nature of the Film, and Application Methodology. Front. Mater. 6:311. doi: 10.3389/fmats.2019.00311

Cleaning is one of the most important and delicate operations in the conservation of cultural heritage, and, if not correctly performed, may irreversibly damage works of art. The removal of aged or detrimental polymeric coatings from works of art is a common operation in conservation, and nanostructured fluids (NSFs), such as aqueous swollen micelles and oil-in-water (o/w) microemulsions, are used as an alternative to non-confined organic solvents, which pose a series of non-negligible drawbacks. NSFs effectiveness in removing polymeric coatings has been thoroughly demonstrated in the last decades, while their cleaning mechanism is still under investigation. The present work deepens the knowledge on the removal mechanisms of NSFs, studying the interaction of a four-component NSF with four different types of acrylic and vinyl polymer films cast from solutions or aqueous polymer latexes on three substrates (glass, marble, and polystyrene) with different hydrophilicity and wettability. NSFs were applied either as non-confined or confined in cellulose poultices (traditionally employed by conservators), or in highly retentive chemical gels, observing the influence of the confining matrix on the removal process. It was found that the NSF/polymer film interaction is greatly dependent on the film structure and composition. Films formed from solvent solutions can be swollen by water/organic solvents mixtures or dewetted when a surfactant is added to the cleaning fluid; films formed from polymer latexes, on the other hand, are generally swollen even just by water alone, but poorly dewet. The substrate also plays an important role in the removal of polymer films formed from solutions, for instance the removal of an acrylic polymer from polystyrene could be achieved only through highly selective cleaning using NSF-loaded chemical hydrogels. These results can be key for conservators, providing innovative solutions to face new challenges in art preservation.

Keywords: polymer coatings, cleaning, nanostructured fluids, acrylics, vinyls, non-ionic surfactants, hydrogels, dewetting

INTRODUCTION

Cleaning of works of art generally consists in the selective removal of materials that promote the degradation of the artifacts or alter their readability and appearance. Among these materials, aged or detrimental polymeric coatings are often found on works of art, and their removal is a common operation in art conservation. Synthetic polymers have been largely employed in the traditional restoration practice as varnishes, adhesives, protectives and consolidating agents. The presence of polymeric coatings on the surface of porous inorganic substrates (wall paintings, stone, mortars) drastically reduces water permeability and enhances the degradation induced by salts, up to consistent loss of the artifacts' surface layers (Carretti and Dei, 2004; Giorgi et al., 2010). Graffiti and vandalism are other well-known examples where selective removal of polymeric coatings must be carried out on artistic surfaces (Apostol et al., 2011; Sanmartín et al., 2014; Giorgi et al., 2017; Baglioni et al., 2018d). Other cases include the removal of aged pressure sensitive tapes from paper artworks (Bonelli et al., 2018), or of discolored and cracked varnishes from paintings (Burnstock and Kieslich, 1996; Baglioni et al., 2018a).

The vast amount of different solvent-sensitive materials found in classic and contemporary art poses continuous challenges to the safe removal of detrimental coatings (Kavda et al., 2017). Traditionally, restorers and conservators rely on the use of organic solvents to dissolve or swell unwanted materials. Solvents are typically applied either as non-confined, using cotton swabs, or thickened in viscous polymeric solutions and solvent gels (Burnstock and Kieslich, 1996; Burnstock and White, 2000; Baglioni et al., 2012c). However, these methods exhibit poor control and scarce selectivity, or involve the presence of residues from the cleaning system. In addition, health concerns arise from the toxicity of most solvents used in restoration.

Alternatively, nanostructured fluids (NSFs) such as aqueous swollen micelles and oil-in-water (o/w) microemulsions were proposed in the late 1980s for the removal of hydrophobic matter from porous inorganic substrates (Borgioli et al., 1995). Their effectiveness in removing polymeric coatings from different types of surfaces has been thoroughly demonstrated in the last decades (Carretti et al., 2003, 2007; Baglioni et al., 2010, 2012b, 2015a,b, 2016, 2018c). These NSFs are water-based systems where limited amounts of solvents are found either in the dispersed (as nano-sized droplets stabilized by surfactants) or in the continuous phase of the fluids. The large surface area developed by the nano-sized droplets, and the synergistic action of solvents and surfactants are responsible for enhanced cleaning power, while the presence of the continuous aqueous phase limits the re-deposition of detached hydrophobic matter on hydrophilic surfaces. Besides, being water-based, aqueous NSFs have reduced toxicity as opposed to traditional solvents. A further improvement was represented by the confinement of NSFs into retentive physical or chemical gels able to gradually release the fluids at the gel-artifact interface, maximizing control over the cleaning action (Baglioni et al., 2015c; Chelazzi et al., 2018).

While these systems represent the most advanced cleaning tools currently available to conservators, the interaction mechanism of NSFs with polymeric coatings is still being investigated.

The removal of high molecular weight macromolecules does not follow the rules of classical detergency. Studies performed on model samples, i.e., glass slides coated with an acrylate copolymer, have shown that dewetting takes place when water-based NSFs are put in contact with the polymeric coating (Raudino et al., 2015, 2017; Baglioni et al., 2017, 2018b). The film swells and detaches from the surface. This behavior was also observed on mortar samples coated with the same polymer (Baglioni et al., 2018b). The nature of both the organic solvents and the surfactant(s) included in the cleaning formulation was found to be of fundamental importance in the whole process. The solvents swell the polymer and lower its glass transition temperature, increasing the mobility of the polymer chains; the surfactant reduces the interfacial tension, kinetically promoting the detachment of the polymer film from the surface, and initiating the dewetting process that eventually breaks down the coating into separate polymer droplets.

Despite providing fundamental insights, previous studies on this subject depicted only a partial picture of the interaction mechanisms between NSFs and polymeric coatings. Namely, all the studies were conducted only on a single type of polymer, i.e., Paraloid B72® (poly(ethyl methacrylate/methyl acrylate) 70:30) cast from solution. Only glass or mortars were considered as substrates. Besides, simplified NSFs formulations were used to isolate the contribution of individual components in the system.

The present work aims to deepen the knowledge on the removal mechanisms of NSFs, studying the interaction of a four-component NSF with four different types of polymer films cast either from solutions or aqueous emulsions. In fact, it is well known that films of polymers cast from solutions have different physical structures than those cast from emulsions (Chevalier et al., 1992; Winnik, 1997; Steward et al., 2000), and polymers emulsions contain several additives; these can be crucial factors in determining the interaction process with the NSFs. For instance, hydrophilic additives in the polymer film might affect the interfacial tensions between the polymer, the substrate, and the NSF, which are key factors in wetting and dewetting processes. Three substrates were considered (glass, marble and polystyrene) with different hydrophilicity and wettability. At this stage, only laboratory samples and non-aged polymers were considered, so as to investigate simpler systems with controlled and known composition. Finally, NSFs were applied either as non-confined or confined in cellulose poultices (traditionally employed by conservators), or in highly retentive chemical gels, observing the influence of the confining matrix on the removal process in terms of controlled release and cleaning effectiveness. Our goal was to use a phenomenological approach to describe qualitatively the interaction between polymer films and NSFs, rather than providing a quantitative evaluation of polymer removal.

The NSF is composed of water, an alcohol ethoxylate nonionic surfactant, 2-butanol (BuOH), and 2-butanone (methyl ethyl ketone, MEK), and is representative of formulations actually employed in the conservation practice for the cleaning of real works of art.

The three selected substrates were coated with the four different polymers, obtaining a set of 12 samples, which were then exposed to the NSF, investigating the interaction mechanism for each combination. The effects of the NSF on the films were studied by means of optical microscopy and micro-reflectance infrared Fourier Transform spectroscopy 2D mapping of the areas of interest, which provides spatial resolution down to the micron-scale.

MATERIALS AND METHODS

Chemicals

$C_{9-11}E_{5,5}$ alcohol ethoxylate (Berol 266, AkzoNobel), sodium dodecylsulfate (SDS, Sigma-Aldrich, purity ≥ 99%), butanone (MEK, Sigma-Aldrich, purity 99%), 2-butanol (BuOH, Sigma-Aldrich, purity 99%), ethanol (EtOH, Fisher Chemical, purity ≥ 99%), white spirit (White Spirit, Fidea), D_2O (EurisoTop, 98%), and deuterated butanone (d-MEK, $C_4H_3D_5O$, Sigma-Aldrich, purity 98%) were used as received, without further purification. Water was purified with a Millipore Milli-Q gradient system (resistance > 18 MΩ cm).

Polymers Formulations

The four polymeric materials selected are widely used in the traditional restoration practice. They include: poly(vinyl acetate) (PVAc), commercially known as PVA K40®, dissolved in ethanol; PVAc as an aqueous emulsion, commercially known as Vinavil NPC®; poly(butyl methacrylate) (PBMA) dissolved in white spirit, commercially known as Plexisol P550®; poly(ethyl acrylate/methyl methacrylate) (PEA/PMMA) 40:60 as an aqueous emulsion, commercially known as Plextol B500®. **Table 1** reports the main properties of the formulations. All the products were applied on the substrates as a 10% (w/w) solution/emulsion.

Differential Scanning Calorimetry (DSC) for the Glass Temperature (Tg) Determination

DSC measurements were performed on a DSC Q1000 from TA Instruments on small samples (2–5 mg) of the four dry films, according to the following procedure: equilibration at −50°C; heating ramp from −50 to 60°C at 10°C/min; cooling ramp from 60 to −50°C at 10°C/min; heating ramp from −50 to 60°C at 10°C/min. The first heating/cooling ramp was used to equilibrate the sample, while the second heating ramp is the one used for the Tg determination. Each sample was run at least twice, in order to check for reproducibility of the measurement.

Substrates

The three different substrates selected for this work, i.e., glass, marble and polystyrene, were selected as they exhibit different wettability and are representative of artistic substrates frequently found in classic or contemporary art production. Glass slides of 5 × 5 × 0.3 cm^3, marble tiles of 5 × 5 × 1 cm^3, and polystyrene slides of 5 × 5 × 0.2 cm^3 were used. The four different filming materials (polymers solutions or emulsions) were then laid manually on the top surfaces of each series of samples. 150 µl of each polymer formulation (V_S, V_E, A_S, A_E) was carefully spread using a pipette on a 4 × 5 cm^2 area on the surface of glass, marble and polystyrene samples. A reference area was thus left untreated. The specimens were left drying for 30 days, and then the dry mass of the films was evaluated. The density of the dry films was then measured, by drying for 4 days in a ventilated oven at 60°C weighed amounts of polymer solutions/emulsions that were poured into graduated vials. The results, reported in **Table 1**, made possible to calculate that the obtained films had an average thickness of ∼5–7 µm, assuming that they are homogeneously spread all over the treated surface.

Attenuated Total Reflectance Fourier-Transform Infrared Spectroscopy

ATR measurements were carried out with a Thermo Nicolet Nexus 870 spectrometer equipped with a liquid nitrogen-cooled MCT detector and a single reflection diamond crystal ATR unit. Spectra were recorded in the 4,000–650 cm^{-1} range (128 scans, 4 cm^{-1} resolution). ATR measurements were performed on small samples of spray-can paints' dried films, removed from the glass support.

NSF Preparation

The NSF selected for this work is composed as follows (w/w): H_2O, 65.9%; $C_{9-11}E_{5,5}$, 3.5%; BuOH, 9.7%; MEK, 20.9%. In order to better understand the role of each component in the interaction with the polymer coatings, other liquid systems were also used, obtained removing some of the components from the complete NSF formulation. Namely, a water/$C_{9-11}E_{5,5}$ surfactant solution, and a water/BuOH/MEK solvents mixture were used. In both systems, the ratio between each component was the same as in the complete NSF formulation. It is worth noting that both BuOH and MEK are partly water-miscible [12.5 and 24% at 20°C, respectively (Verschueren, 2001)] and this made possible to obtain a single-phase stable mixture of water and solvents even in the absence of surfactants.

Small-Angle Neutron Scattering

Small-angle neutron scattering (SANS) experiments were performed on the spectrometer V4 (Bensc-Helmholtz Zentrum Berlin). Two different configurations were employed (i.e., sample-to-detector distances, SD = 2 or 8 m) to cover a range of wave vectors q [$q = (4\pi/\lambda)\sin(\theta/2)$, where λ is the wavelength of the incident neutron beam and θ the scattering angle] from 0.007 to 0.28 $Å^{-1}$. For each configuration a 6 Å neutron wavelength was used and the wavelength resolution, $\Delta\lambda/\lambda$, was <10%. Samples were contained in 1 mm thick quartz cells and kept at 20 ± 2°C during the measurements. The scattering intensity was corrected for the empty cell contribution, transmission, and detector efficiency and was normalized to the absolute scale by direct measurement of the intensity of the incident neutron beam. The integration of the normalized 2D intensity distribution with respect to the azimuthal angle yielded the 1D scattering intensity distribution, $I(q)$, in cm^{-1}. The reduction of the data was performed using standard BENSC procedures for small-angle isotropic scattering. The background from the incoherent scattering coming from each sample was determined from analysis of the Porod asymptotic limit and subtracted from the normalized spectra. Experimental data normalized to absolute scale were fitted using Igor routines (NCNR_SANS_

TABLE 1 | Main properties and sample names of the four commercial polymers used.

Commercial name	Polymer nature	Physical appearance	Dry matter content	Applied as	Sample name[a]	Film density (g/cm^3)[b]	Tg (°C)[c]
PVA K40®	PVAc	Transparent grains	–	10% solution in EtOH	V_S	1.27	31
Vinavil NPC®	PVAc	Aqueous emulsion	52%	10% aqueous emulsion	V_E	1.05	16
Plexisol P550®	PBMA	40% solution in white spirit	40%	10% solution in white spirit	A_S	1.08	28
Plextol B500®	PEA/PMMA	Aqueous emulsion	50%	10% aqueous emulsion	A_E	1.03	30

[a] *V, vinyl; A, acrylic; S, polymer applied as a solution; E, polymer applied as an emulsion.*
[b] *The density was calculated as described in section Substrates.*
[c] *The glass temperature (Tg) was measured by means of DSC analyses according to the procedure described in section Differential Scanning Calorimetry (DSC) for the Glass Temperature (Tg) Determination.*

package_6.011) (Kline, 2006) available from NIST, National Institute for Standard and Technology, Gaithersburg, MD, running on Igor Pro© (Wavemetric Inc., Lake Oswego, Oregon; Version 6.22).

NSF/Polymer Interaction Experiments

Immersion Tests

The aim of these tests was to investigate the direct interaction between cleaning fluids and polymer films, without the influence of a medium (i.e., cellulose pulp poultice or gel). To this purpose, the coated specimens were partly immersed in about 30 ml of the selected fluids, i.e., the minimum amount of fluid needed to treat the samples. The area of the polymer film exposed to the fluid action was kept constant and fixed to 1 × 5 cm^2. At selected time intervals, up to 10 min, the specimens were extracted from the fluid and let dry, and then visual inspection of possible changes in the film was carried out. At $t = 0$ min and $t = 10$ min the superficial micromorphology of the films (after drying) was investigated by optical microscopy and FTIR 2D micro-reflectance mapping. Finally, after 10 min of incubation with each liquid system, a removal test was performed on all the samples, using a cotton swab soaked with water, in order to check the removability of the polymeric coatings.

Confocal Laser Scanning Microscopy (CLSM)

Confocal Microscopy experiments were performed on a Leica TCS SP8 confocal microscope (Leica Microsystems GmbH, Wetzlar, Germany) equipped with a 63× water immersion objective. The four polymers were stained with Coumarin 6, which was dissolved/dispersed in the liquid solutions or latexes. Then, 2–4 μm-thick polymer films were obtained by spin coating coverglasses for 60 s at 1,000 rpm. Coumarin 6 was excited with the 488 nm laser line of an argon laser. The emission of the dye was acquired with a PMT in the range 498–530 nm. CLSM experiments were performed to monitor the interaction of the different polymer films with the NSF. Briefly, 50 μl of the unlabeled liquid phase were put in contact with the coumarin 6-labeled polymer coated coverglass, and the morphological variations of the polymeric film were monitored over time.

Cleaning Tests

Two sets of cleaning tests were performed, in order to evaluate the influence on the application method of the NSF, and the effect of the supporting material (i.e., cellulose pulp poultice or chemical hydrogel) on the interaction between the NSF and the polymeric coating. Traditional cellulose pulp poultices were prepared by mixing 35 mg of cellulose pulp (Arbocel®, Zecchi, Firenze) and 160 μl of NSF. The obtained poultices were applied, interposing a Japanese paper sheet (Zecchi, Firenze) between the compress and the specimen surface, on 1 cm^2 areas of each sample for 15 min. After removing the poultices, a gentle mechanical action was performed on the treated surface, by means of wet cotton swabs. Poly(hydroxyethyl methacrylate/poly vinylpyrrolydone) semi-interpenetrated networks (pHEMA/PVP SIPNs) are highly retentive hydrogels, previously proposed in combination with NSFs for the cleaning of works of art (Baglioni et al., 2018a), and prepared as described elsewhere (Domingues et al., 2013a,b). Gels having a size of 1 × 1 × 0.2 cm^3 were used, able to upload ca. 160 μl of NSF, i.e., the same amount of cleaning fluid loaded in the poultices. The gels were loaded with the NSFs by immersion for 24 h, so as to exchange water within the gel with the NSFs. The gel was applied for 15 min, and at the end of the treatment a gentle mechanical action was performed on the coating residues.

Contact Angle Measurements

The contact angle of 5 μL sessile droplets of Milli-Q water on the selected material surface was measured with a Rame-Hart Model 190 CA Goniometer. The three substrates and the four polymer films were investigated. The equilibrium contact angle was measured in at least eight different areas, and the average value and standard deviation was evaluated.

Optical Microscopy

A Reichert Zatopan 353–890 microscope was used to collect micrographs. The instrument was coupled with a Nikon Digital Sight DS-Fi2 camera. The NIS-ELEMENTS software was used to capture and edit images.

Fourier-Transform Infrared Spectroscopy–2D Micro-Reflectance Mapping

The Fourier transform infrared (FTIR) 2D imaging of the treated surfaces was carried out using a Cary 620–670 FTIR microscope, equipped with an FPA 128 × 128 detector (Agilent Technologies). The spectra were recorded directly on the surface of the samples in reflectance mode, with open aperture and

TABLE 2 | Contact angle of water droplets on the surface of the four selected polymeric coatings, and of the three types of substrates.

Sample	Contact angle	Substrate	Contact angle
V_S	57.8 ± 0.8°	glass	35.3 ± 3.1°
V_E	39.1 ± 1.9°	marble	61.7 ± 1.8°
A_S	78.2 ± 3.1°	polystyrene	77.0 ± 1.6°
A_E	62.5 ± 2.1°		

a spectral resolution of 8 cm^{-1}, acquiring 128 scans for each spectrum. Each analysis produces an IR map of 700 × 700 μm^2 (128 × 128 pixels), with a spatial resolution of 5.5 μm (i.e., each pixel has dimensions of 5.5 × 5.5 μm^2 and is associated to an independent spectrum). In each map, the intensity of a characteristic peak of each polymer, e.g., the C=O ester stretching typical of both acrylics and vinyls, at about 1,730 cm^{-1}, was shown with a chromatic scale, following the order red > yellow > green > blue.

RESULTS AND DISCUSSION

Polymer Films Characterization

The four polymeric coatings were characterized by means of FTIR-ATR and contact angle measurements. **Table 2** reports the values for the contact angle of water droplets laid on the surface of the polymer films, or of the selected substrates (glass, marble, polystyrene). The substrates exhibit a range of contact angles passing from hydrophilic (glass) to hydrophobic surfaces (polystyrene). Regarding the polymers, it can be noticed that the acrylics are more hydrophobic than the vinyls, and the films deriving from polymer latexes are more hydrophilic than those coming from solutions. This is likely due to the presence of surfactants, stabilizers, and other polar additives in the latexes emulsions, which affect the wettability of the film.

Figure 1 shows the FTIR-ATR spectra of the four polymer films. The spectra of the two vinyl films match closely, confirming that the same type of polymers is present in both films. The main bands were assigned as follows (Doménech-Carbó et al., 2001; Learner and Institute, 2004): C-H stretching (2,928 cm^{-1} and a shoulder at 2,972 cm^{-1}); C=O stretching (intense and narrow peak at 1,727 cm^{-1}); asymmetric stretching of the C–O group (1,222 cm^{-1}, distinctive of PVAc); C–H in-plane bending (1,428 cm^{-1} and 1,371 cm^{-1}); C–H out-of-plane bending (1,117 cm^{-1}); C–O symmetric stretching (1,018 cm^{-1}); C–C stretching (944 cm^{-1}); C–H rocking (792 cm^{-1}). Besides, the spectrum of V_E shows a broad band at 3,335 cm^{-1}, which is likely due to the OH stretching of poly(vinyl alcohol) (PVA), i.e., one of the main additives of the Vinavil NPC® aqueous latex.

The spectra of A_S and A_E show slightly different features in the fingerprint and CH stretching regions, as expected given the different type of acrylate polymers found in those films.

The main bands of the acrylic films were assigned as follows (Doménech-Carbó et al., 2001; Learner and Institute, 2004; Pintus and Schreiner, 2011): C–H stretching (A_S: peaks at 2,958, 2,933, 2,873 cm^{-1}; A_E: peaks at 2,887 cm^{-1} and 2,860 cm^{-1}); C=O stretching (1,720 cm^{-1}); C–H in-plane bending (1,465 and 1,380 cm^{-1}; A_E shows an additional peak is visible at 1,343 cm^{-1}); C–O stretching (A_S: peaks at 1,240 and 1,065 cm^{-1}; A_E: peaks at 1,279, 1,241, 1,109, and 1,022 cm^{-1}); C–C stretching (965 and 946 cm^{-1}); C–H rocking (840 and 750 cm^{-1}).

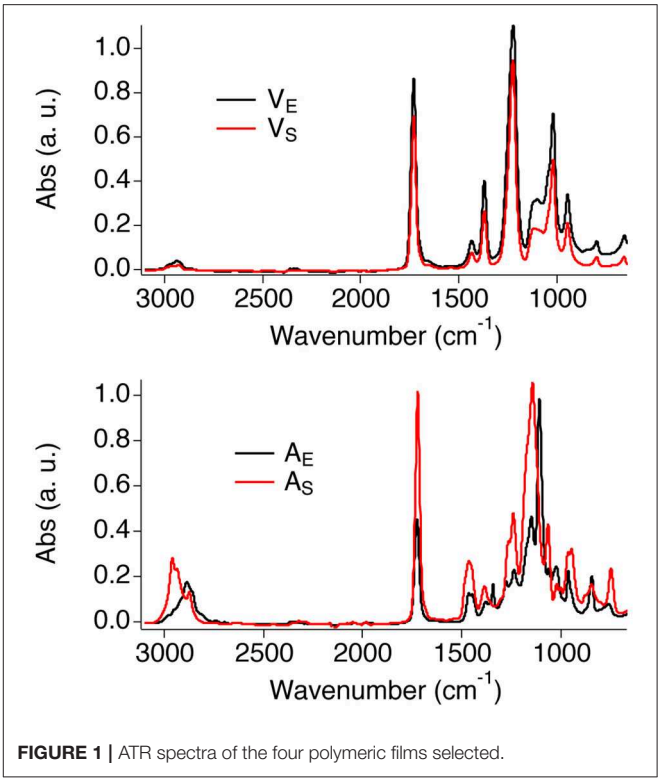

FIGURE 1 | ATR spectra of the four polymeric films selected.

NSF Characterization

The selected NSF for this work is composed of water, a nonionic surfactant and two solvents, i.e., BuOH and MEK, which are partly miscible with water. The structure of this NSF was never studied before, thus acquiring information on the micelles' size and shape, and on the location of each component in the NSF, was deemed a preliminary step to help understanding the interaction of the fluid with the polymeric films. To this aim, SANS measurements were performed on four D_2O based samples: (1) the $D_2O/C_{9-11}E_{5.5}$ binary mixture; (2) the $D_2O/C_{9-11}E_{5.5}$/BuOH ternary system; (3) the complete NSF formulation, i.e., $D_2O/C_{9-11}E_{5.5}$/BuOH/MEK; (4) the complete NSF formulation with deuterated d-MEK fully replacing the regular MEK. The analysis of samples 3 and 4 represents a contrast variation experiment, in which everything is kept constant from one sample to the other, except for its contrast, by changing the scattering length density (SLD) of one or more chemicals (in this case, exchanging MEK with d-MEK).

Figure 2-top shows the SANS profiles for the four samples analyzed. The data were fitted according to two different models. The supramolecular aggregates, in the case of the binary surfactant/water and the water/surfactant/BuOH systems, were modeled as non-interacting polydisperse core-shell spheres, defined by two contrasts, i.e., bulk/shell and shell/core. On the other hand, the best fitting for the complete NSF was obtained by modeling the micelles as non-interacting prolate core-shell

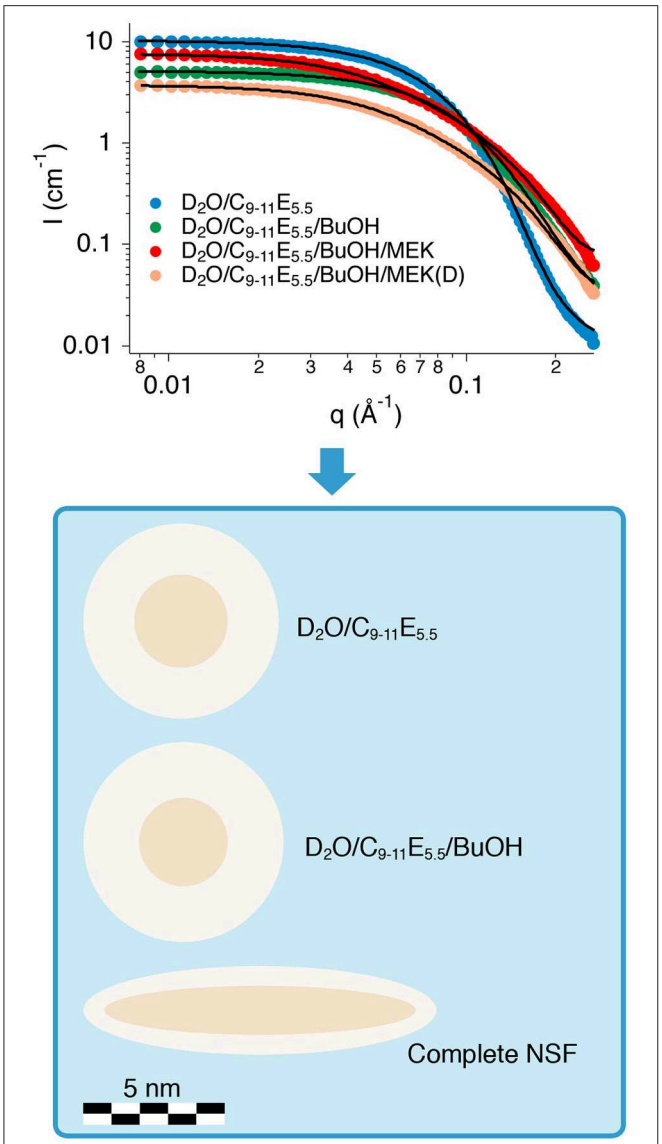

FIGURE 2 | (Top) SANS profiles of the four samples analyzed. The best fitting curves are represented as continuous black lines. (Bottom) The cartoon illustrates the structural evolution (in scale) of the three formulations investigated, i.e., the binary water/surfactant mixture, the water/surfactant/alcohol system, and the complete NSF.

ellipsoidal particles, again defined by a double contrast. The SLD of bulk, shell and core, i.e., respectively, ρ_{bulk}, ρ_{shell}, and ρ_{core}, were calculated according to the SLD for neutrons of each chemical included in the formulations, as reported in **Table 3**. For globular micelles of homogeneous scattering length density, the total scattered intensity $I(q)$ (cm^{-1}) is given by (Sheu and Chen, 1988; Liu et al., 1995):

$$I\left(q\right) = N_P V_P^2 \Delta\rho^2 P\left(q\right) S\left(q\right) + bkg_{inc} \quad (1)$$

TABLE 3 | SLD for neutrons scattering of the chemicals included in the NSF.

Chemical formula/structure	Compound/molecular group	SLD (10^{-6} Å^{-2})
D_2O	Heavy water	6.39
$CH_3(CH_2)_{8-10}(OCH_2CH_2)_{5.5}OH$	$C_{9-11}E^a_{5.5}$	0.37
$CH_3(CH_2)^a_{8-10}$	$C_{9-11}E_{5.5}$ apolar tail	−0.41
$HO(CH_2CH_2O)_{5.5}$	$C_{9-11}E_{5.5}$ polar head	0.97
$C_4H_{10}O$	BuOH	−0.33
$C_4H_3D_5O$	d-MEK	3.66
C_4H_8O	MEK	0.17

[a]*For the SLD calculation a C_{10} aliphatic chain was considered.*

where N_p is the number density of the scattering particles (cm^{-3}), V_p is the volume (cm^3), $\Delta\rho$ is the contrast term (cm^{-2}), $P(q)$ is the form factor, and $S(q)$ is the structure factor. In this case $S(q) = 1$, as the particles were considered to be non-interacting. In the case of spherical core-shell aggregates, the particle scattering intensity is expressed as follows (Kline, 2006):

$$I\left(q\right) = \frac{\phi}{V_P}\left[\left(\rho_{core}-\rho_{shell}\right)\frac{3V_c j\left(qr_c\right)}{qr_c} + \left(\rho_{shell}-\rho_{bulk}\right)\frac{3V_P j(qr_s)}{qr_s}\right]^2 \quad (2)$$

where $j(x)$ is a spherical Bessel function and is expressed as:

$$j\left(x\right) = \frac{\left(\sin x - x\cos x\right)}{x^2} \quad (3)$$

and where φ is the volume fraction of the micellar phase, V_c is the core volume, r_c is the core radius, $r_s = r_c + t$ (t is the shell thickness). Since this model takes into account a polydisperse core, which follows the Schultz distribution, the form factor calculated in Equation (2) is normalized by the average particle volume:

$$\langle V\rangle = \frac{4\pi}{3}\left\langle r_c^3\right\rangle \quad (4)$$

where:

$$\left\langle r_c^3\right\rangle = \frac{(z+2)(z+3)}{(z+1)^2}\left\langle r_c\right\rangle \quad (5)$$

and z is the width parameter of the Schultz distribution (Degiorgio et al., 1985):

$$z = \frac{1}{\left(\frac{\sigma}{\langle r_c\rangle}\right)^2} - 1 \quad (6)$$

being σ^2 the variance of the distribution. The polydispersity index (PDI), reported in **Table 4** is defined as $\sigma/\langle r_c\rangle$ [see equation (6)] and its value is comprised between 0 and 1.

In the case of monodisperse non-interacting prolate ellipsoids, on the other hand, when modeling asymmetric micelles with a

TABLE 4 | Fitting results of the SANS data acquired on the NSF.

Fitting parameter	$D_2O/C_{9-11}E_{5.5}$	$D_2O/C_{9-11}E_{5.5}$/BuOH	Complete NSF
r (Å)	16.7 ± 0.3	15.7 ± 0.2	–
t (Å)	17.9 ± 0.1	19.6 ± 0.1	9.4 ± 0.4
PDI	0.20 ± 0.01	0.40 ± 0.02	–
a (Å)	–	–	53.0 ± 2.0
b (Å)	–	–	7.2 ± 0.3
P_{BuOH}	–	0.30 ± 0.03	0.28 ± 0.02
P_{MEK}	–	–	0.17 ± 0.01

core-shell scattering length profile, $P(q)$ included in Equation (1) is usually calculated as an orientationally-averaged normalized form factor, $\overline{P}(q)$. First, the orientation-dependent form factor $F(q, \mu)$, is defined as follows (where μ is the cosine between the direction of the symmetry axis of the ellipsoid and the Q vector):

$$F\left(q,\mu\right) = f\left(\rho\right)\frac{3j\left(u\right)}{u} + \left(1 - f\left(\rho\right)\right)\frac{3j\left(v\right)}{v} \tag{7}$$

where $j(x)$ is the same spherical Bessel function defined in Equation (3) and u and v are expressed as:

$$u = q[\mu^2 a^2 + (1-\mu^2)b^2]^{1/2} \tag{8}$$

$$v = q[\mu^2 (a+t)^2 + (1-\mu^2)(b+t)^2]^{1/2} \tag{9}$$

which define the geometrical shape of the micelles, and where $f(\rho)$ contains the contrast calculation, and a, b, t are the geometrical parameters of the ellipsoid, i.e., the major semi-axis, the minor semi-axis, and the shell thickness, respectively.

$\overline{P}(q)$ is then calculated as follows (Kotlarchyk and Chen, 1983):

$$\overline{P}\left(q\right) = \int_0^1 d\mu \left|F(q,\mu)\right|^2 \tag{10}$$

Even though the measured samples included D_2O instead of H_2O, the structural picture emerging from the analysis of SANS data can be safely transferred to the H_2O-based NSF, apart from possible slight changes (Baglioni et al., 2012a).

Table 4 shows the main fitting results, while **Figure 2**-bottom contains a cartoon depicting the size and shape evolution of micelles following the addition of each component to the formulation. The size of $C_{9-11}E_{5.5}$ micelles in D_2O was perfectly consistent with the length of the surfactant molecule and with the results of previous SAXS measurements performed on similar systems (Baglioni et al., 2017), where a $r + t$ total micelle radius of about 35 Å had been obtained. A polydispersity index of 0.2 for the size of the hydrophobic core fits such systems, which usually have a PDI in the 0.1–0.5 range. According to fitting results, the structure and size of the micelles do not change significantly after the addition of BuOH (see **Figure 2**-bottom). In fact, BuOH was found to be partitioned between the micellar and the aqueous bulk phase in a 30:70 ratio, meaning that most of the solvent is mixed with water. The fraction solubilized in the micelles is preferentially located in the shell, replacing D_2O hydration molecules, and thus affects the micellar size and shape only slightly. The main effect of the inclusion of BuOH is to double the polydispersity of the core radius with respect to the binary water/surfactant system, even though the value is perfectly suitable for a micellar solution.

The results of the contrast variation experiments performed on the complete NSF formulation showed that the inclusion of a significant amount of MEK in the system completely alters both the size and shape of the aggregates (see **Figure 2**-bottom), as the result of a sphere-to-rod transition. This behavior was observed for similar systems containing the same surfactant (Baglioni et al., 2014) and is likely due to the system getting closer to its cloud point. In fact, micelles are known to grow and assume elongated shapes close to the clouding temperature, as observed in the present case. $C_{9-11}E_{5.5}$ has a cloud point of about 55–60°C, which is known to be lowered by the interaction of this surfactant with MEK (Baglioni et al., 2014). The inclusion of MEK in the system does not alter significantly the partition coefficient of BuOH (P_{BuOH}) between the micelles and the water phase, while MEK is mainly dissolved in the bulk phase ($P_{MEK} = 0.17$).

Overall, SANS analysis clarified that the structure of the NSF is that of rod-like micelles, mainly composed of the sole surfactant, dispersed in a water/solvents mixture, indicating that the system is close to its cloud point. This structural information has relevant implications in terms of cleaning power of the NSF, as detergency is known to be maximized when these systems are close to the cloud point (Holmberg, 2002; Holmberg et al., 2002; Stubenrauch, 2008; Baglioni et al., 2014). Therefore, high cleaning effectiveness was expected from this NSF formulation.

NSF/Polymer Interaction

The interaction between the NSF and the four polymer films was initially investigated simply by immersing the coated specimens into four different liquid systems, i.e., water, water/surfactant, water/solvents, and the complete NSF. The micromorphology of the film was observed by optical microscopy at different times during the total 10 min of incubation of the specimens in the liquids, while 2D micro-FTIR mapping was performed on the polymer surface before exposure to the fluids and after 10 min of incubation. Finally, a removal test was performed on the polymers using wet cotton swabs, in order to check their removability.

Looking at the results of the immersion tests, illustrated in **Figures 3**–**6** and summarized in **Table 5**, a clear difference in the behavior of samples emerges, i.e., the polymer films deriving from latexes (V_E and A_E) are preferentially swollen and only in few cases partly dewetted, whereas the films deriving from solutions are unaffected by just water, are swollen by the surfactant solution, and are partly or completely dewetted when solvents are included in the liquid systems. For instance, **Figures 3**, **5** show how for chemically identical polymers (both PVAc) the type of the film plays a key role in determining the behavior when the film is exposed to the same NSF. 2D microFTIR mapping was crucial to confirm the location and distribution of the polymers on the micron-scale. In particular, when a film is

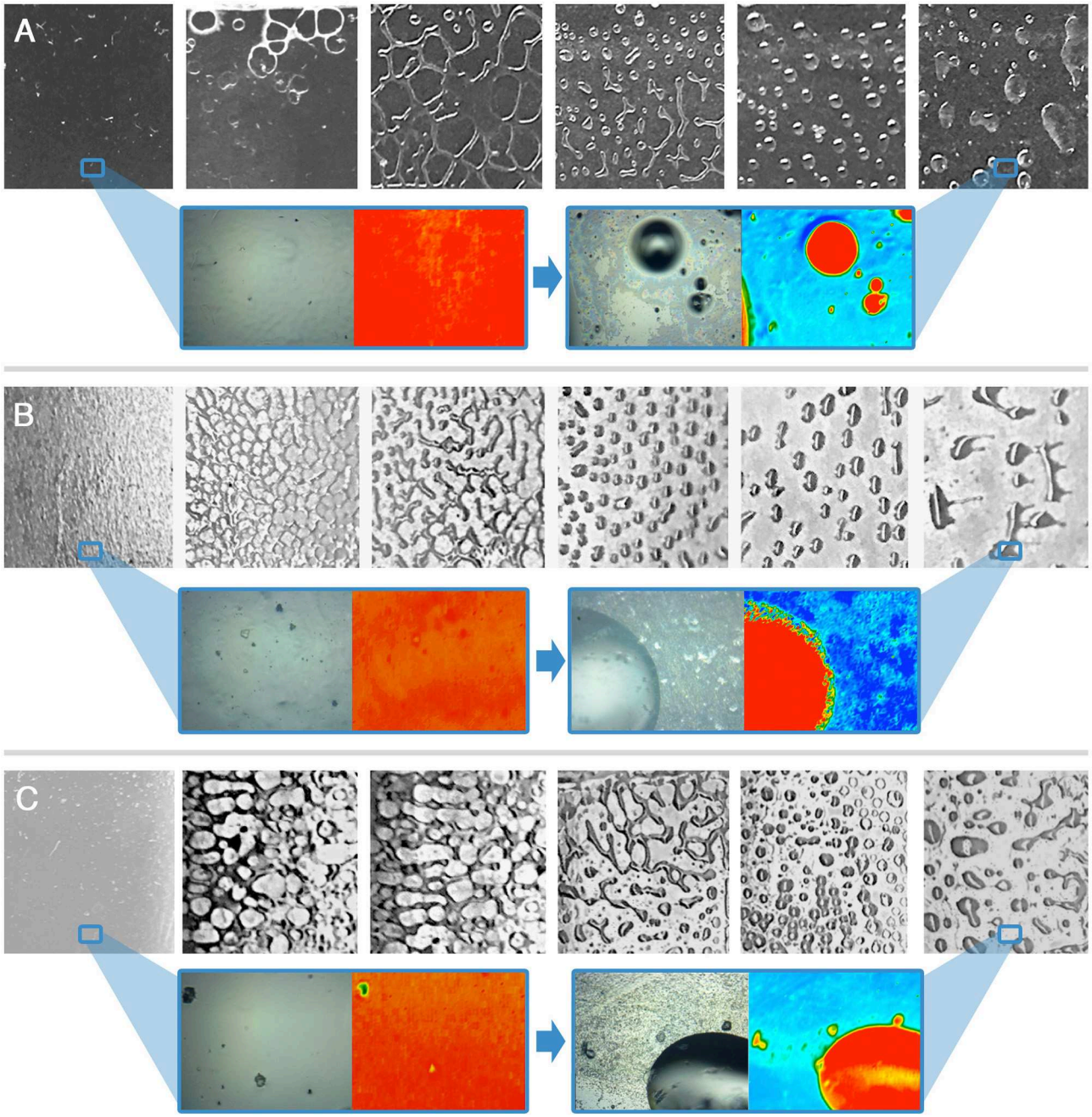

FIGURE 3 | Immersion tests results for the V_S-coated glass **(A)**, marble **(B)**, and polystyrene **(C)** specimens. The frames, left to right, are taken at $t = 0$ s, 10 s, 30 s, 1 min, 5 min, 10 min. For $t = 0$ s and $t = 10$ min a representative 2D micro-reflectance FTIR map is reported, together with its relative micrograph in visible light. In each map, the intensity of the C=O ester stretching at about 1,730 cm^{-1} is shown with a chromatic scale, following the order red > yellow > green > blue. Visible light micrographs are approximately 1 cm^2 large; the FTIR mapping areas have a size of 400 μm × 550 μm. The blue boxes highlight areas of the samples, which were investigated by 2D FTIR mapping; the position of the blue frame in the lower magnification images does not correspond to the actual position of the investigated areas.

dewetted (see **Figures 3**, **4**) it was shown that no polymer residues are present (above the instrumental detection limit) outside the droplets on the substrate surface. In fact, it has been shown that the detection limit of an FPA detector is significantly lower than that of conventional mercury cadmium telluride (MCT) detectors for the FTIR detection of trace amounts of materials. The heterogeneous distribution of analytes can result in small areas of localized high concentration, which can be detected thanks to the high spatial resolution of the FPA detector (Chan and Kazarian, 2006). For instance, for polyvinyl alcohol and

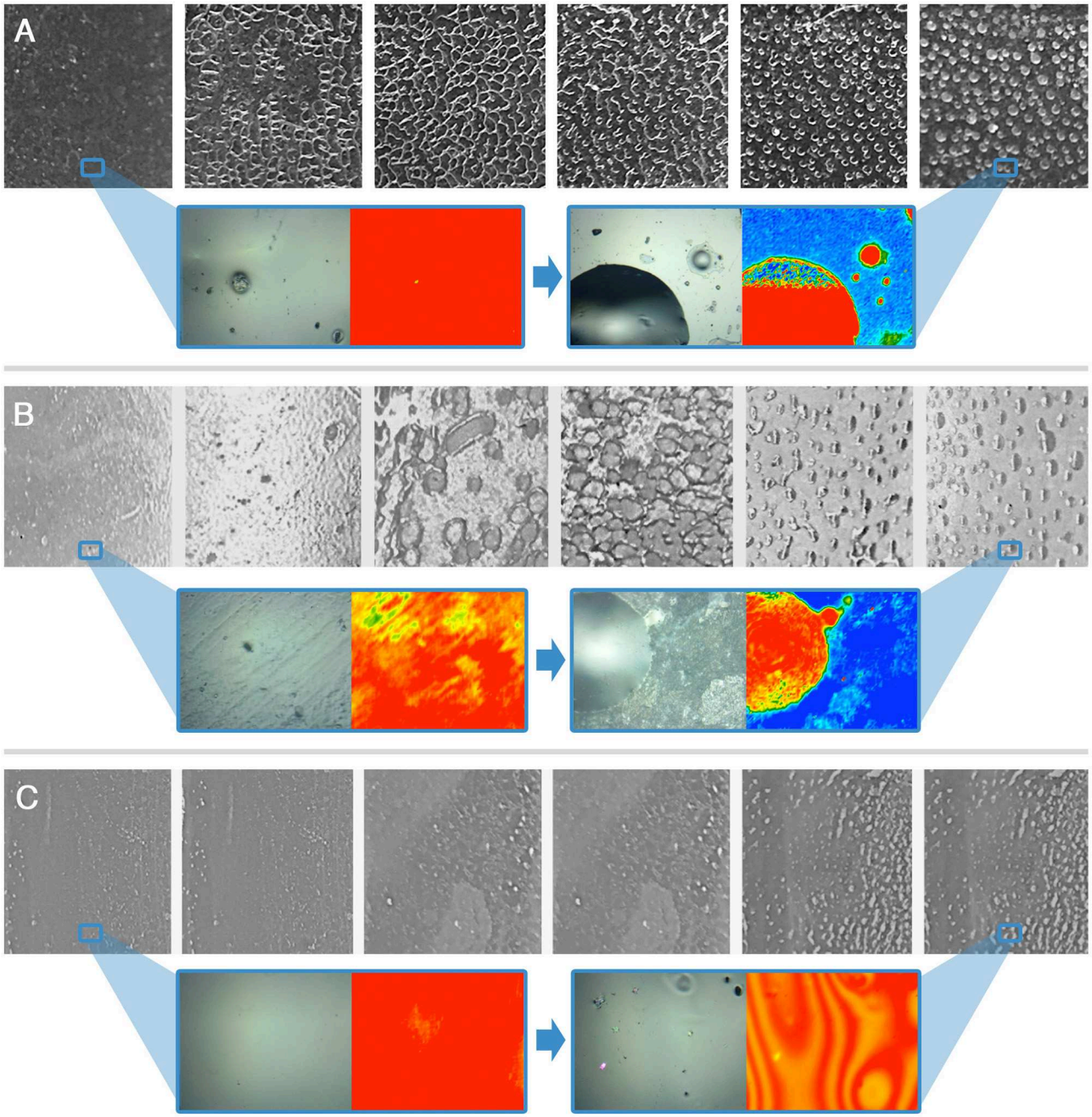

FIGURE 4 | Immersion tests results for the A_S-coated glass **(A)**, marble **(B)**, and polystyrene **(C)** specimens. The frames, left to right, are taken at $t = 0$ s, 10 s, 30 s, 1 min, 5 min, 10 min. For $t = 0$ s and $t = 10$ min a representative 2D micro-reflectance FTIR map is reported, together with its relative micrograph in visible light. In each map, the intensity of the C=O ester stretching at about 1,730 cm^{-1} is shown with a chromatic scale, following the order red > yellow > green > blue. Visible light micrographs are approximately 1 cm^2 large; the FTIR mapping areas have a size of 400 μm × 550 μm. The blue boxes highlight areas of the samples, which were investigated by 2D FTIR mapping; the position of the blue frame in the lower magnification images does not correspond to the actual position of the investigated areas.

polyvinyl acetate we verified that quantities < 1 pg/pixel (1 pixel = 5.5 × 5.5 μm) can be detected.

Polymer coatings formed from aqueous emulsions are significantly more sensitive to the action of water [a well-known issue when emulsion-based acrylic paint layers are exposed to aqueous cleaning fluids (Murray et al., 2002; Ormsby and Learner, 2009; Willneff et al., 2014)], and tend to be swollen. This is justified by the presence of a non-negligible amount of hydrophilic additives and surfactants in the polymer emulsions, which remain in the film after drying and are able to interact with

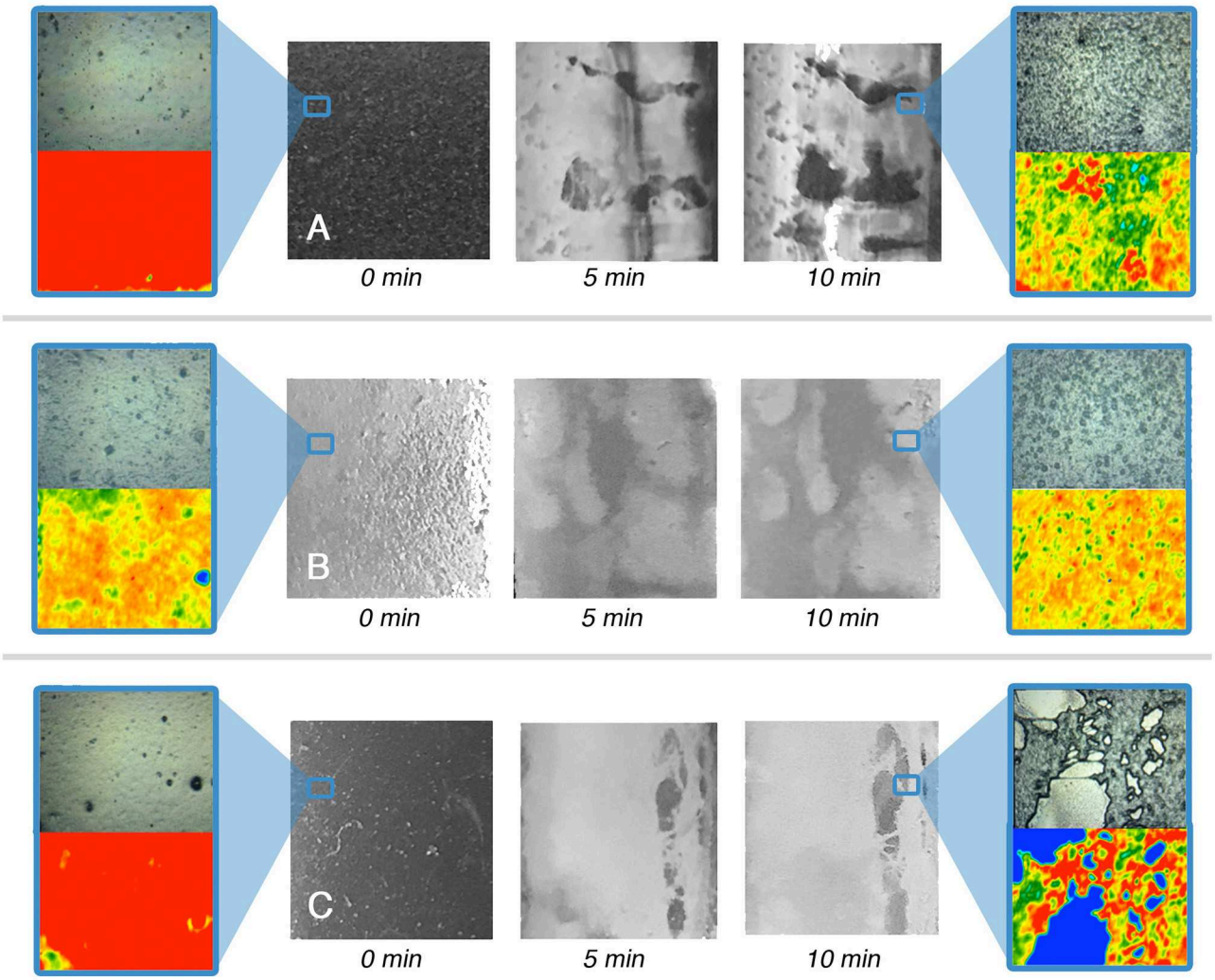

FIGURE 5 | Immersion tests results for the V_E-coated glass **(A)**, marble **(B)**, and polystyrene **(C)** specimens. For $t = 0$ s and $t = 10$ min a representative 2D micro-reflectance FTIR map is reported, together with its relative micrograph in visible light. In each map, the intensity of the C=O ester stretching at about 1,730 cm^{-1} is shown with a chromatic scale, following the order red > yellow > green > blue. Visible light micrographs are approximately 1 cm^2 large; the FTIR mapping areas have a size of 400 μm × 550 μm. The blue boxes highlight areas of the samples, which were investigated by 2D FTIR mapping; the position of the blue frame in the lower magnification images does not correspond to the actual position of the investigated areas.

water molecules, favoring the swelling of the film. The presence of hydrophilic additives can also explain why the swollen films tend to dewet less easily. The energetic balance of dewetting can be described by the spreading coefficient S, which for a polymer film on a glass surface, immersed in a liquid, is defined as (Baglioni and Chelazzi, 2013):

$$S = \gamma_{LG} - \gamma_{PG} - \gamma_{LP} \quad (11)$$

where γ_{LG} is the interfacial tension between glass and the liquid, γ_{PG} is the interfacial tension between glass and the polymer, and γ_{LP} is the interfacial tension between the liquid and the polymer. When S is negative, dewetting is energetically favored and occurs spontaneously unless an activation energy barrier hinders the process kinetically. Hydrophilic additives in the polymer film might lower the values of both γ_{PG} and γ_{LP}, making S less negative for a given liquid/polymer/glass set. On the other hand, the presence of surfactant additives may lower the glass transition temperature (T_g) of the polymer films (as in the case of V_E–see **Table 1**), making polymer chains more mobile, thus possibly decreasing the energy costs related to the formation of new interfacial regions during the detachment of the film, and lowering the activation energy necessary to initiate dewetting (Baglioni et al., 2017, 2018b; Montis et al., 2019).

Overall, in the case of the polymer films from emulsions investigated here, the films' thermodynamic stability seems to prevail on the kinetic drive of the dewetting process. However, the swollen films are softened and easily removable from glass and marble even with water and water/$C_{9-11}E_{5.5}$, meaning that the adhesion to the solid surface was sensibly reduced,

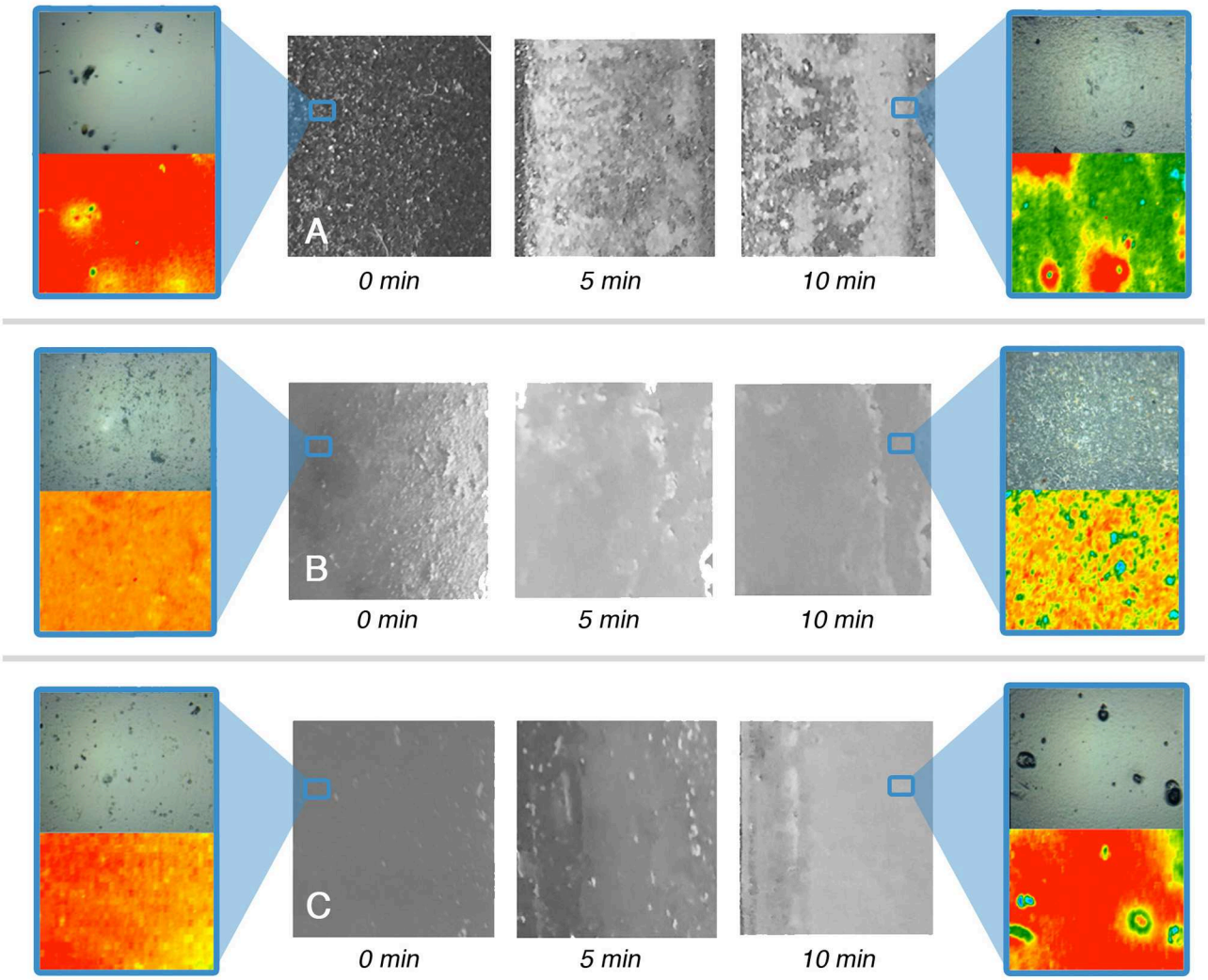

FIGURE 6 | Immersion tests results for the A_E-coated glass **(A)**, marble **(B)**, and polystyrene **(C)** specimens. For $t = 0$ s and $t = 10$ min a representative 2D micro-reflectance FTIR map is reported, together with its relative micrograph in visible light. In each map, the intensity of the C=O ester stretching at about 1,730 cm^{-1} is shown with a chromatic scale, following the order red > yellow > green > blue. Visible light micrographs are approximately 1 cm^2 large; the FTIR mapping areas have a size of 400 μm × 550 μm. The blue boxes highlight areas of the samples, which were investigated by 2D FTIR mapping; the position of the blue frame in the lower magnification images does not correspond to the actual position of the investigated areas.

while in the case of polystyrene the removal is slightly more difficult. When a polymer film formed from a solvent solution is exposed to a cleaning fluid, a more diversified behavior is observed. Water and water/$C_{9-11}E_{5.5}$ are partly or completely ineffective in removing the films. Instead, dewetting processes are induced by water/solvents mixtures or, more efficiently, by the synergistic action of solvents and surfactants (Gentili et al., 2012; Xu et al., 2012; Baglioni et al., 2017, 2018b). This is clearly exemplified by A_S on marble, where water alone produces no visible effects on the polymer. The nonionic surfactant micellar solution is able to induce some swelling of the film, but not sufficient to grant its easy removal. A water/solvents mixture, on the other hand, produces a partial dewetting pattern, and the film can be partly removed using some mechanical action. This means that solvents are able to swell the polymer to such an extent that the T_g is lowered below room temperature, starting the dewetting process. However, it is only with the synergistic action of a surfactant, which lowers the interfacial tension at the liquid/substrate and liquid/polymer interfaces, that dewetting proceeds further, leading to easy and complete polymer removal. The substrate's chemical nature is a key factor. Increasing the hydrophobicity of the substrate, the affinity of the polymer film with the substrate increases, leading to less efficient polymer removal, culminating with the limit case of A_S on polystyrene, which resulted completely irremovable.

The interaction between the complete NSF and the four polymer films was also monitored through CLSM imaging, as described in section Confocal Laser Scanning Microscopy

TABLE 5 | Results of immersion tests performed on polymer-coated glass, marble and polystyrene specimens.

		Glass		Marble		Polystyrene	
		Film appearance	**Removability[a]**	**Film appearance**	**Removability[a]**	**Film appearance**	**Removability[a]**
V_S	H_2O	No change	±	No change	x	No change	x
	$H_2O/C_{9-11}E_{5.5}$	Swollen	o	Swollen	±	Swollen	±
	H_2O/BuOH/MEK	Dewetted	o	Dewetted	o	Dewetted	o
	NSF	Dewetted	o	Dewetted	o	Dewetted	o
A_S	H_2O	No change	x	No change	x	No change	x
	$H_2O/C_{9-11}E_{5.5}$	Swollen	o	Swollen	x	Swollen	x
	H_2O/BuOH/MEK	Dewetted	o	Partly dewetted	±	Swollen	x
	NSF	Dewetted	o	Dewetted	o	Swollen	x
V_E	H_2O	Swollen	o	Swollen	o	Partly dewetted	o
	$H_2O/C_{9-11}E_{5.5}$	Swollen	o	Swollen	o	Partly dewetted	o
	H_2O/BuOH/MEK	Swollen	o	Swollen	o	Swollen	±
	NSF	Swollen	o	Swollen	o	Partly dewetted	o
A_E	H_2O	Swollen	o	Swollen	o	Swollen	o
	$H_2O/C_{9-11}E_{5.5}$	Swollen	o	Swollen	o	Swollen	o
	H_2O/BuOH/MEK	Swollen	o	Swollen	o	Swollen	±
	NSF	Swollen	o	Swollen	o	Swollen	o

Both the film appearance and its removability after 10 min of incubation in the four different liquid systems are summarized in the table, following analysis with optical microscopy and 2D micro-FTIR mapping.

[a]After 10 min of incubation in the liquid systems, the removability of the coatings was checked performing a gentle mechanical action with a cotton swab soaked with water; x, no removal; ±, partial removal; o, complete removal.

(CLSM). Homogeneous and reproducible 2–4 μm thick films on coverglasses were obtained by spin coating. **Figure 7** summarizes the results of the investigation, which were in perfect agreement with what was observed during the immersion tests reported above. A_S and V_S, i.e., the polymer films cast from solutions, were completely and quickly dewetted by the NSF, while A_E and V_E, i.e., the films cast from polymer latexes, were just swollen. **Figure 7** shows that some small cracks and/or holes (of few microns) are visible in the V_E and A_E swollen films, which nonetheless maintain their overall coherence on a macro-scale. These holes possibly form in correspondence of previous film defects, which can be present on such thin films. Overall, the behavior of polymer films cast from aqueous latexes can be seen as if the physical process stopped at the very early stages of dewetting. This is in agreement with what observed during previous experiments, and seems to enforce the hypothesis that the amphiphilic additives in these films play a key role in inhibiting the dewetting process, which otherwise would likely occur.

The inhomogeneous aspect of the V_E and A_E films at $t = 0$ is due to the fact that the hydrophobic fluorescent dye was not evenly distributed in the aqueous polymer latex. As the films is swollen by the penetration of the organic solvents, the dye evenly spread through the film.

CLSM investigations, overall, allowed to confirm the results of the immersion tests on macroscopic samples, where the polymer thickness could not be directly measured and not accurately controllable.

Finally, the influence of the application methodology on the outcome of removal tests was evaluated. To this aim, the same amount of NSF was uploaded, respectively, in traditional cellulose pulp poultices and in pHEMA/PVP chemical hydrogels. The latter have been characterized and assessed in the last years, and their use for the removal of unwanted materials from water-sensitive substrates has been thoroughly reported (Domingues et al., 2013a; Baglioni et al., 2018a; Bonelli et al., 2018). Recently, SAXS and rheology studies showed that these gels act as "sponges," able to load different NSFs without being altered or dramatically alter the properties of the fluids (Baglioni et al., 2018a).

The two systems were applied for 15 min on the surface of the films, and then micrographs of the treated area were taken before checking the coating removability via gentle mechanical action with a wet cotton swab. As visible in **Figure 8**, the areas treated with the NSF-loaded poultice are generally more inhomogeneous than the ones treated with the NSF-loaded hydrogel. Moreover, several cellulose fibers were spotted on the samples that were in contact with the poultice, indicating the permanence of paper or cellulose pulp residues on the treated areas. Dewetting patterns could be clearly highlighted in the areas of A_S on glass and marble treated with the NSF-loaded hydrogel, indicating a more controlled and reliable cleaning action. In any case, after the removal of either the compress or the gel, complete and easy removal could be obtained via a gentle mechanical action using wet cotton swabs, for all the specimens except A_S on polystyrene. In this case, the acrylic polymer could not be removed after 15 min of application of either the NSF-loaded poultice or hydrogel (**Figures 9A,B**). We hypothesized that in this case the application time was too long, causing the migration of solvents through the A_S coating up to the polymer/substrate interface,

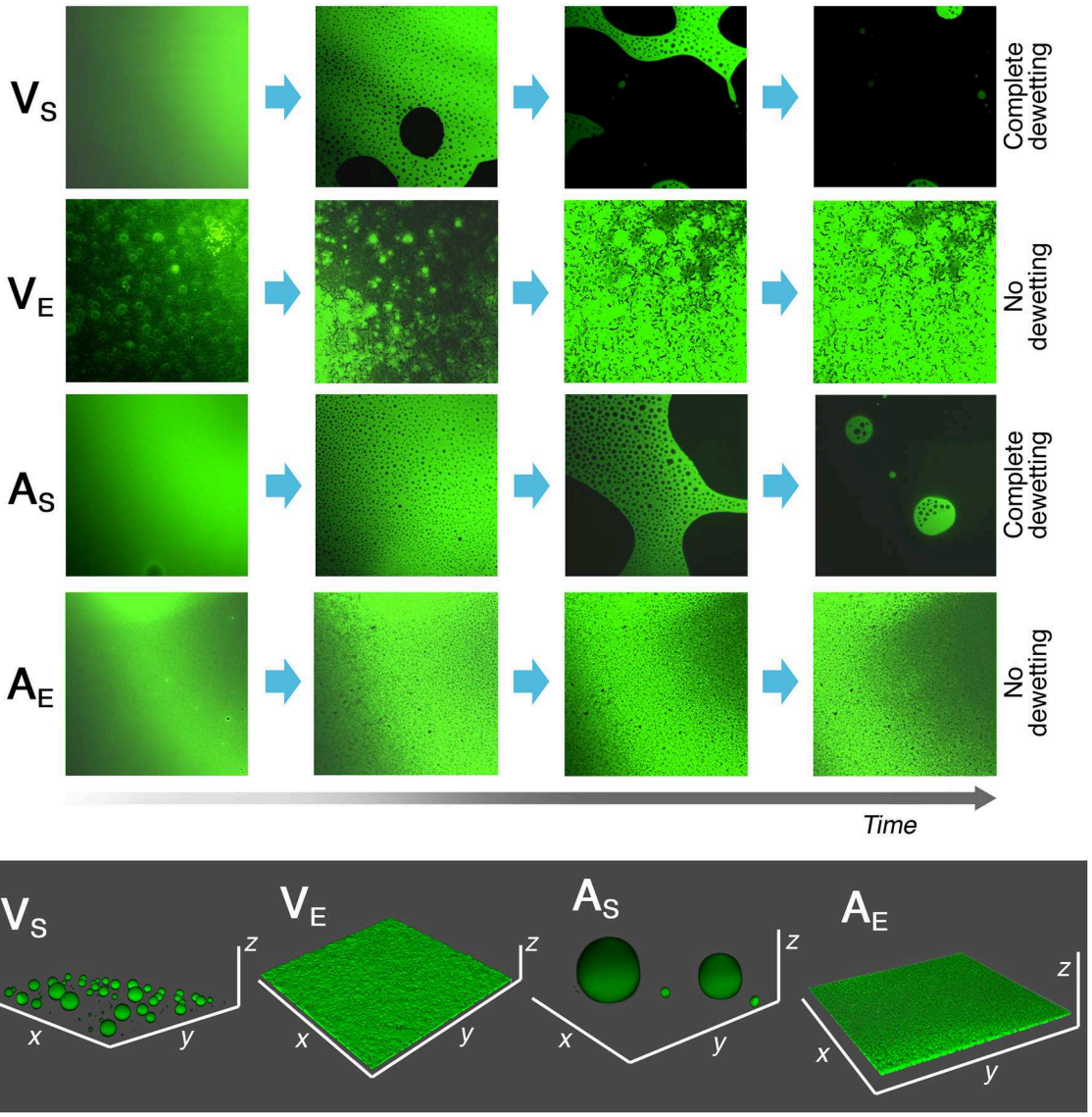

FIGURE 7 | Results of CLSM experiments on 2–4 μm thick spin-coated polymer films on coverglasses. The films were exposed to the action of 50 μl of the NSF, and their morphology was observed over time. The time scale is not the same for all samples, i.e., V_S and A_S completely dewetted from the coverglass in less than 10 s, while V_E and A_E films were still intact after 10 minutes of incubation with the NSF. In the bottom gray box, the 3D reconstruction of the four polymers' morphology after 10 min is reported. The different behavior between polymer films coming from solvent solutions or aqueous emulsions is clearly evidenced. Each side of the CLSM micrographs is 150 μm long. *x* and *y* axes in the 3D reconstructions have the same length.

where they interacted with polystyrene creating a sort of joint or adhesion layer between the polymer and the substrate. This issue is easily overcome by using multiple shorter applications, assuming that the confining matrix of the NSF is enough retentive to release gradually the uploaded fluid on short time scales, which is the case of the pHEMA/PVP gels. In fact, repeated shorter applications (2 +2 +2 min) of the NSF loaded in the hydrogel allowed complete removal of the coating (as confirmed by the 2D microFTIR mapping), while uneven polymer residues were left from the same application using cellulose poultices (see **Figures 9C–F)**. The cartoon in **Figure 9** summarizes the removal process in the two cases: using the highly retentive hydrogel it is possible to perform a gradual action, which proceeds layer by layer, controlling the interaction of the NSF with the substrate. This approach was recently used to perform highly selective removal of overpaintings and vandalism (Giorgi et al., 2017). It is worth noting that the pHEMA/PVP gels used for cleaning interventions do not leave detectable residues on the treated surfaces (as checked with FTIR), while the only non-volatile residues in the NSFs (i.e., the surfactants) can be feasibly removed with a rinsing steps using the gels simply loaded with water (Baglioni et al., 2016).

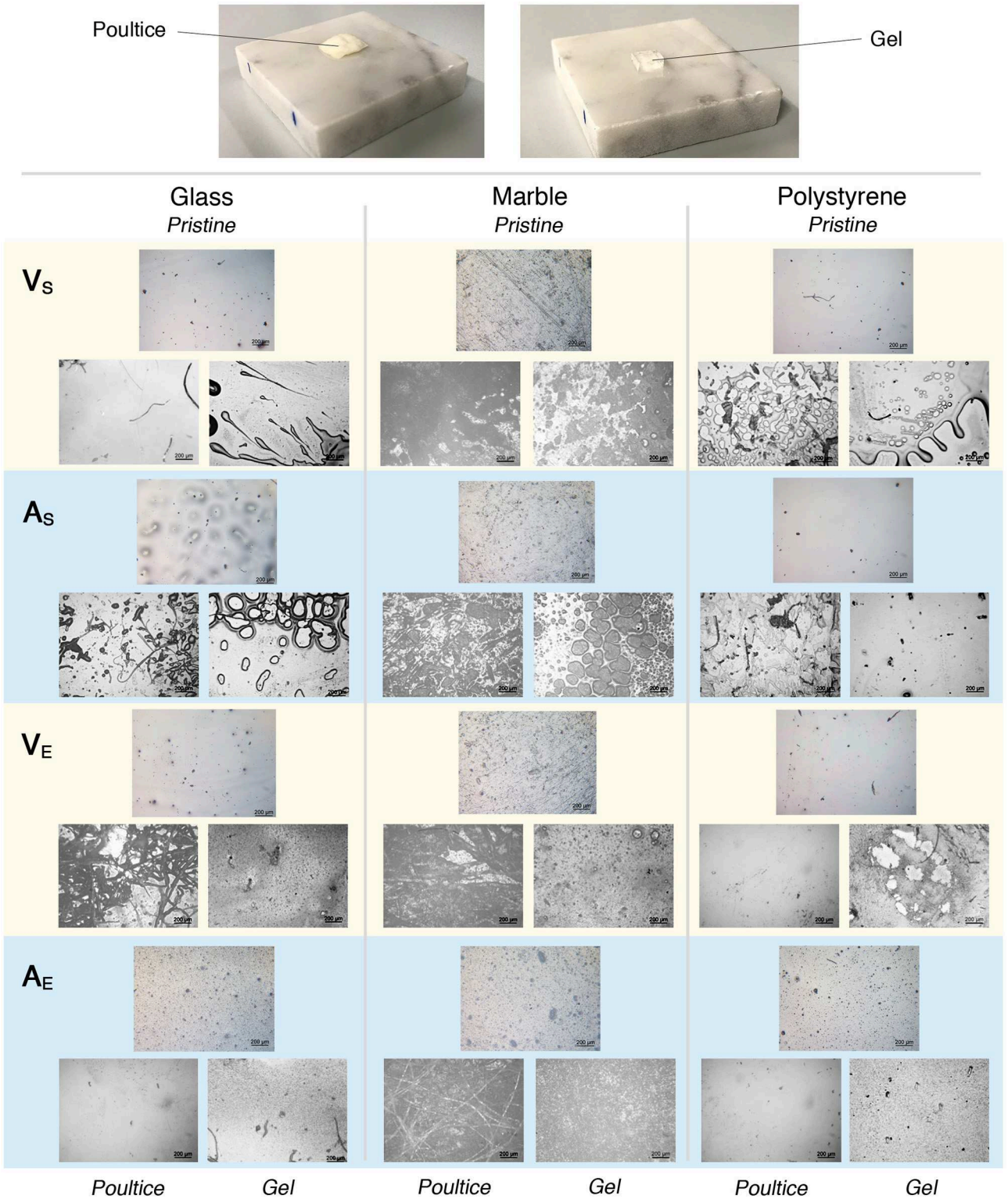

FIGURE 8 | Results of the cleaning tests performed comparing the effect of the same amount of NSF loaded respectively on a traditional cellulose pulp poultice and on an innovative highly retentive chemical hydrogel. (Top) Marble specimens during the tests. (Bottom) Selected representative micrographs taken before (*Pristine*, top-middle picture of each triad) and after 15 min of application of both the poultice (bottom-left picture of each triad) and the gel (bottom-right picture of each triad). Each micrograph is 1.2 × 1.6 mm^2 large.

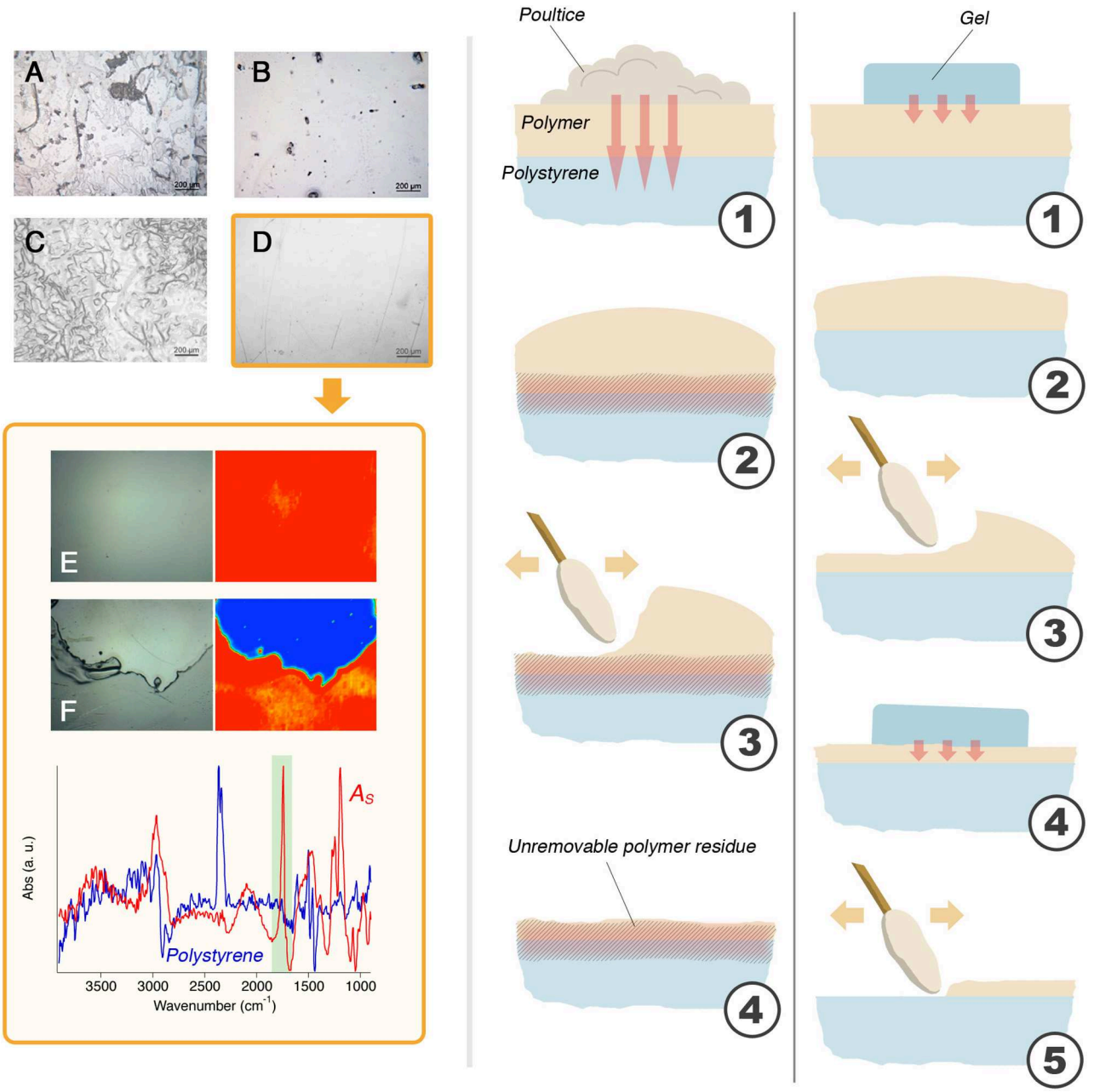

FIGURE 9 | (A) The result of 15 min of application of the NSF-loaded poultice on A_S laid on polystyrene; **(B)** The result of 15 min of application of the NSF-loaded gel on A_S laid on polystyrene; **(C)** The result of 2 min + 2 min + 2 min of application of the NSF-loaded poultice on A_S laid on polystyrene; **(D)** The result of 2 min + 2 min + 2 min of application of the NSF-loaded gel on A_S laid on polystyrene. This is the only case that resulted in the complete removal of the polymer coating, as confirmed by the comparison between the micro-reflectance FTIR maps collected before **(E)** and after **(F)** the cleaning with the NSF-loaded hydrogel (the micro-picture is taken at the border between of the cleaned area, seen in blue). The cartoon on the right illustrates the mechanism proposed to explain the observed results. With the poultice (left), the solvents migrate through the polymer (1) and attack the polystyrene substrate, creating a junction or an enhanced adherence between the polymer film and the substrate (2). When a mechanical action is performed (3), an uneven layer of unremoved polymer layer is left stuck to the surface of polystyrene. Using the gel (right), the solvents migration is limited by the retention properties of the scaffold (1). The outer layers of the polymer coating are, then, slightly swollen (2) and easily removed by means of a gentle mechanical action (3). The gel is applied again (4) and the removal proceeds layer by layer, in a selective way, which allows for the complete and safe removal of the polymer film (5). Micrographs A, B, C, and D are 1.2 × 1.6 mm^2 large; micrographs E and F (and relative FTIR maps) have a size of 400 × 550 µm.

CONCLUSIONS

This study focused on unveiling some key aspects of the NSFs/polymer coatings interaction depending on several different factors: (i) the chemical nature and, thus, hydrophilicity of the substrate; (ii) the chemical nature and physical structure of the polymeric films to be removed; (iii) the influence of the application methodology on the cleaning outcome. A series of systematic tests was performed and a coherent and clear picture emerged. A water/C_{9-11}E5.5/BuOH/MEK NSF was selected for this study and was firstly characterized by means of SANS measurements, which showed that rod-like nonionic micelles are dispersed in a water/BuOH/MEK mixture close to the system cloud point. These features possibly make this NSF particularly effective in polymer removal. Then, glass, marble, and polystyrene specimens were coated with four different polymers, including two vinyls and two acrylics, each applied either as a solvent solution or as an aqueous emulsion. It was found that the NSF/polymer film interaction is greatly dependent on the film structure and composition. Films formed from solvent solutions can be swollen by water/organic solvents mixtures or dewetted when a surfactant is added to the cleaning fluid; films formed from polymer latexes, on the other hand, are generally swollen even just by water, but they tend not to dewet. This happens independently from the chemical nature of the polymer, and is a direct consequence of its structure and composition, which includes a significant amount of amphiphilic additives. These substances alter the energetic balance of the liquid/polymer/solid system and stabilize the film, which does not dewet. However, the films are easily removable from the substrates, meaning that the action of the cleaning fluid induces loss of adhesion, similarly to what happens during the first stages of the dewetting process that occurs for films cast from polymer solutions. The substrate also plays an important role in the removal of polymer films formed from solutions. In particular, the more the film is affine to the substrate, the harder its removal. In the limit case, the removal of an acrylic polymer from polystyrene could be achieved only through selective cleaning action using a NSF-loaded highly retentive chemical hydrogel, which grants significantly more controlled performances than traditional cellulose pulp poultices. These results have 2-fold relevance: they deepen the knowledge of the physico-chemical processes that underpin phenomena of daily conservation practice, and provide conservators with innovative solutions to face new challenges in art preservation.

DATA AVAILABILITY STATEMENT

The datasets generated for this study will not be made publicly available. The relevant data are already completely and clearly reported in the paper.

AUTHOR CONTRIBUTIONS

MB, MA, DC, and RG contributed to the conception and design of the work, to the acquisition, the analysis, and the interpretation of experimental data. PB and RG revised the work critically giving a substantial intellectual contribution, and ultimately provided the final approval for its publication.

FUNDING

This work was supported by the European Union (CORDIS)–Project NANORESTART (H2020-NMP-21-2014/646063) and PRIN 2017–MIUR. The access to SANS facilities has been supported by the European Commission under the 7th Framework Programme through the Key Action: Strengthening the European Research Area, Research Infrastructures, contract no. 226507 (NMI3).

ACKNOWLEDGMENTS

Dr. Uwe Keiderling was kindly acknowledged for his assistance during SANS experiments performed at the HZB.

REFERENCES

Apostol, I., Damian, V., Garoi, F., Iordache, I., Bojan, M., Apostol, D., et al. (2011). Controlled removal of overpainting and painting layers under the action of UV laser radiation. *Opt. Spectrosc.* 111:287. doi: 10.1134/S0030400X11080054

Baglioni, M., Bartoletti, A., Bozec, L., Chelazzi, D., Giorgi, R., Odlyha, M., et al. (2016). Nanomaterials for the cleaning and pH adjustment of vegetable-tanned leather. *Appl. Phys. A* 122:114. doi: 10.1007/s00339-015-9553-x

Baglioni, M., Berti, D., Teixeira, J., Giorgi, R., and Baglioni, P. (2012a). Nanostructured surfactant-based systems for the removal of polymers from wall paintings: a small-angle neutron scattering study. *Langmuir* 28, 15193–15202. doi: 10.1021/la303463m

Baglioni, M., Domingues, J. A. L., Carretti, E., Fratini, E., Chelazzi, D., Giorgi, R., et al. (2018a). Complex fluids confined into semi-interpenetrated chemical hydrogels for the cleaning of classic art: a rheological and SAXS study. *ACS Appl. Mater. Interfaces* 10, 19162–19172. doi: 10.1021/acsami.8b01841

Baglioni, M., Giorgi, R., Berti, D., and Baglioni, P. (2012b). Smart cleaning of cultural heritage: a new challenge for soft nanoscience. *Nanoscale* 4:42–53. doi: 10.1039/C1NR10911A

Baglioni, M., Jàidar Benavides, Y., Berti, D., Giorgi, R., Keiderling, U., and Baglioni, P. (2015a). An amine-oxide surfactant-based microemulsion for the cleaning of works of art. *J. Colloid Interface Sci.* 440, 204–210. doi: 10.1016/j.jcis.2014.10.003

Baglioni, M., Jáidar Benavides, Y., Desprat-Drapela, A., and Giorgi, R. (2015b). Amphiphile-based nanofludis for the removal of styrene/acrylate coatings: cleaning of stucco decoration in the Uaxactun archeological site (Guatemala). *J. Cult. Herit.* 16, 862–868. doi: 10.1016/j.culher.2015.03.008

Baglioni, M., Montis, C., Brandi, F., Guaragnone, T., Meazzini, I., Baglioni, P., et al. (2017). Dewetting acrylic polymer films with water/propylene carbonate/surfactant mixtures – implications for cultural heritage conservation. *Phys. Chem. Chem. Phys.* 19, 23723–23732. doi: 10.1039/C7CP02608K

Baglioni, M., Montis, C., Chelazzi, D., Giorgi, R., Berti, D., and Baglioni, P. (2018b). Polymer film dewetting by water/surfactant/good-solvent mixtures: a mechanistic insight and its implications for the conservation

of cultural heritage. *Angew. Chem. Int. Ed. Engl.* 57, 7355–7359. doi: 10.1002/anie.201710930

Baglioni, M., Poggi, G., Ciolli, G., Fratini, E., Giorgi, R., and Baglioni, P. (2018c). A Triton X-100-based microemulsion for the removal of hydrophobic materials from works of art: SAXS characterization and application. *Materials* 11:E1144. doi: 10.3390/ma11071144

Baglioni, M., Poggi, G., Jaidar Benavides, Y., Martínez Camacho, F., Giorgi, R., and Baglioni, P. (2018d). Nanostructured fluids for the removal of graffiti – A survey on 17 commercial spray-can paints. *J. Cult. Herit.* 34, 218–226. doi: 10.1016/j.culher.2018.04.016

Baglioni, M., Raudino, M., Berti, D., Keiderling, U., Bordes, R., Holmberg, K., et al. (2014). Nanostructured fluids from degradable nonionic surfactants for the cleaning of works of art from polymer contaminants. *Soft Matter* 10, 6798–6809. doi: 10.1039/C4SM01084A

Baglioni, M., Rengstl, D., Berti, D., Bonini, M., Giorgi, R., and Baglioni, P. (2010). Removal of acrylic coatings from works of art by means of nanofluids: understanding the mechanism at the nanoscale. *Nanoscale* 2, 1723–1732. doi: 10.1039/c0nr00255k

Baglioni, P., Berti, D., Bonini, M., Carretti, E., Del Carmen Casas Perez, M., Chelazzi, D., et al. (2012c). Gels for the conservation of cultural heritage. *MRS Online Proc. Libr.* 1418. doi: 10.1557/opl.2012.97

Baglioni, P., Carretti, E., and Chelazzi, D. (2015c). Nanomaterials in art conservation. *Nat. Nanotechnol.* 10, 287–290. doi: 10.1038/nnano.2015.38

Baglioni, P., and Chelazzi, D. (2013). *Nanoscience for the Conservation of Works of Art*. Cambridge, UK: RSC Publishing. doi: 10.1039/9781849737630

Bonelli, N., Montis, C., Mirabile, A., Berti, D., and Baglioni, P. (2018). Restoration of paper artworks with microemulsions confined in hydrogels for safe and efficient removal of adhesive tapes. *Proc. Natl. Acad. Sci.* 115, 5932–5937. doi: 10.1073/pnas.1801962115

Borgioli, L., Caminati, G., Gabrielli, G., and Ferroni, E. (1995). Removal of hydrophobic impurities from pictorial surfaces by means of heterogeneous systems. *Sci. Technol. Cult. Herit. J.* 4, 67–74.

Burnstock, A., and Kieslich, T. (1996). *A Study of the Clearance of Solvent Gels Used for Varnish Removal From Paintings*. London: James & James, 253–262.

Burnstock, A., and White, R. (2000). A preliminary assessment of the aging/degradation of ethomeen C-12 residues from solvent gel formulations and their potential for inducing changes in resinous paint media. *Stud. Conserv.* 45, 34–38. doi: 10.1179/sic.2000.45.Supplement-1.34

Carretti, E., and Dei, L. (2004). Physicochemical characterization of acrylic polymeric resins coating porous materials of artistic interest. *Prog. Org. Coat.* 49, 282–289. doi: 10.1016/j.porgcoat.2003.10.011

Carretti, E., Dei, L., and Baglioni, P. (2003). Solubilization of acrylic and vinyl polymers in nanocontainer solutions. *Appl. Microemulsions Micelles Cult. Herit. Conserv. Langmuir* 19, 7867–7872. doi: 10.1021/la034757q

Carretti, E., Giorgi, R., Berti, D., and Baglioni, P. (2007). Oil-in-water nanocontainers as low environmental impact cleaning tools for works of art: two case studies. *Langmuir* 23, 6396–6403. doi: 10.1021/la700487s

Chan, K. L. A., and Kazarian, S. G. (2006). Detection of trace materials with Fourier transform infrared spectroscopy using a multi-channel detector. *Analyst* 131, 126–131. doi: 10.1039/B511243E

Chelazzi, D., Giorgi, R., and Baglioni, P. (2018). Microemulsions, micelles, and functional gels: how colloids and soft matter preserve works of art. *Angew. Chem. Int. Ed Engl.* 57, 7296–7303. doi: 10.1002/anie.201710711

Chevalier, Y., Pichot, C., Graillat, C., Joanicot, M., Wong, K., Maquet, J., et al. (1992). Film formation with latex particles. *Colloid Polym. Sci.* 270, 806–821. doi: 10.1007/BF00776153

Degiorgio, V., Corti, M., and Società italiana di fisica. (1985). *Physics of Amphiphiles–Micelles, Vesicles, and Microemulsions: Varenna on Lake Como, Villa Monastero, 19–29 July 1983*. Amsterdam: North-Holland Publishing.

Doménech-Carbó, M. T., Doménech-Carbó, A., Gimeno-Adelantado, J. V., and Bosch-Reig, F. (2001). Identification of synthetic resins used in works of art by fourier transform infrared spectroscopy. *Appl. Spectrosc.* 55, 1590–1602. doi: 10.1366/0003702011954152

Domingues, J., Bonelli, N., Giorgi, R., and Baglioni, P. (2013b). Chemical semi-IPN hydrogels for the removal of adhesives from canvas paintings. *Appl. Phys. A* 114, 705–710. doi: 10.1007/s00339-013-8150-0

Domingues, J. A. L., Bonelli, N., Giorgi, R., Fratini, E., Gorel, F., and Baglioni, P. (2013a). Innovative hydrogels based on semi-interpenetrating p(HEMA)/PVP networks for the cleaning of water-sensitive cultural heritage artifacts. *Langmuir* 29, 2746–2755. doi: 10.1021/la3048664

Gentili, D., Foschi, G., Valle, F., Cavallini, M., and Biscarini, F. (2012). Applications of dewetting in micro and nanotechnology. *Chem. Soc. Rev.* 41, 4430–4443. doi: 10.1039/c2cs35040h

Giorgi, R., Baglioni, M., and Baglioni, P. (2017). Nanofluids and chemical highly retentive hydrogels for controlled and selective removal of overpaintings and undesired graffiti from street art. *Anal. Bioanal. Chem.* 409, 3707–3712. doi: 10.1007/s00216-017-0357-z

Giorgi, R., Baglioni, M., Berti, D., and Baglioni, P. (2010). New methodologies for the conservation of cultural heritage: micellar solutions, microemulsions, and hydroxide nanoparticles. *Acc. Chem. Res.* 43, 695–704. doi: 10.1021/ar900193h

Holmberg, K. (2002). *Handbook of Applied Surface and Colloid Chemistry*. Hoboken, NJ: John Wiley and Sons.

Holmberg, K., Jönsson, B., Kronberg, B., and Lindman, B. (2002). *Surfactants and Polymers in Aqueous Solution*. Hoboken, NJ: John Wiley and Sons. doi: 10.1002/0470856424

Kavda, S., Richardson, E., and Golfomitsou, S. (2017). The use of solvent-gel systems for the cleaning of PMMA. *MRS Adv.* 2, 2179–2187. doi: 10.1557/adv.2017.249

Kline, S. R. (2006). Reduction and analysis of SANS and USANS data using IGOR Pro. *J. Appl. Crystallogr.* 39, 895–900. doi: 10.1107/S0021889806035059

Kotlarchyk, M., and Chen, S. H. (1983). Analysis of small angle neutron scattering spectra from polydisperse interacting colloids. *J. Chem. Phys.* 79, 2461–2469. doi: 10.1063/1.446055

Learner, T., and Institute, G. C. (2004). *Analysis of Modern Paints*. Los Angeles, CA: Getty Publications.

Liu, Y. C., Ku, C. Y., LoNostro, P., and Chen, S. H. (1995). Ion correlations in a micellar solution studied by small-angle neutron and x-ray scattering. *Phys. Rev. E* 51, 4598–4607. doi: 10.1103/PhysRevE.51.4598

Montis, C., Koynov, K., Best, A., Baglioni, M., Butt, H. J., Berti, D., et al. (2019). Surfactants mediate the dewetting of acrylic polymer films commonly applied to works of art. *ACS Appl. Mater. Interfaces* 11, 27288–27296. doi: 10.1021/acsami.9b04912

Murray, A., Berenfeld, C. C., de, Chang, S. Y. S., Jablonski, E., Klein, T., Riggs, M. C., et al. (2002). The condition and cleaning of acrylic emulsion paintings. *MRS Online Proc. Libr. Arch.* 712. doi: 10.1557/PROC-712-II1.4

Ormsby, B., and Learner, T. (2009). The effects of wet surface cleaning treatments on acrylic emulsion artists' paints – a review of recent scientific research. *Rev. Conserv.* 10, 29–41. doi: 10.1179/sic.2009.54.Supplement-1.29

Pintus, V., and Schreiner, M. (2011). Characterization and identification of acrylic binding media: influence of UV light on the ageing process. *Anal. Bioanal. Chem.* 399, 2961–2976. doi: 10.1007/s00216-010-4357-5

Raudino, M., Giamblanco, N., Montis, C., Berti, D., Marletta, G., and Baglioni, P. (2017). Probing the cleaning of polymeric coatings by nanostructured fluids: A QCM-D study. *Langmuir* 33, 5675–5684. doi: 10.1021/acs.langmuir.7b00968

Raudino, M., Selvolini, G., Montis, C., Baglioni, M., Bonini, M., Berti, D., et al. (2015). Polymer films removed from solid surfaces by nanostructured fluids: microscopic mechanism and implications for the conservation of cultural heritage. *ACS Appl. Mater. Interfaces* 7, 6244–6253. doi: 10.1021/acsami.5b00534

Sanmartín, P., Cappitelli, F., and Mitchell, R. (2014). Current methods of graffiti removal: a review. *Constr. Build. Mater.* 71, 363–374. doi: 10.1016/j.conbuildmat.2014.08.093

Sheu, E. Y., and Chen, S. H. (1988). Thermodynamic analysis of polydispersity in ionic micellar systems and its effect on small-angle neutron scattering data treatment. *J. Phys. Chem.* 92, 4466–4474. doi: 10.1021/j100326a044

Steward, P. A., Hearn, J., and Wilkinson, M. C. (2000). An overview of polymer latex film formation and properties. *Adv. Colloid Interface Sci.* 86, 195–267. doi: 10.1016/S0001-8686(99)00037-8

Stubenrauch, C. (2008). *Microemulsions: Background, New Concepts, Applications, Perspectives*. Hoboken, NJ: John Wiley and Sons.

Verschueren, K. (2001). *Handbook of Environmental Data on Organic Chemicals*. Hoboken, NJ: John Wiley and Sons.

Willneff, E. A., Schroeder, S. L., and Ormsby, B. A. (2014). Spectroscopic techniques and the conservation of artists' acrylic emulsion paints. *Herit. Sci.* 2:25. doi: 10.1186/s40494-014-0025-y

Winnik, M. A. (1997). Latex film formation. *Curr. Opin. Colloid Interface Sci.* 2, 192–199. doi: 10.1016/S1359-0294(97)80026-X

Xu, L., Sharma, A., and Joo, S. W. (2012). Dewetting of stable thin polymer films induced by a poor solvent: role of polar interactions. *Macromolecules* 45, 6628–6633. doi: 10.1021/ma30 1227m

Conflict of Interest: The authors declare that the research was conducted in the absence of any commercial or financial relationships that could be construed as a potential conflict of interest.